Geotechnical Aspects of Underground Construction in Soft Ground – Yoo, Park, Kim & Ban (Eds)

Application of close range photogrammetry to passive and active retaining wall model tests and numerical analysis

Suk-Min Kong & Yong-Joo Lee
Department of Civil Engineering, Seoul National University of Science & Technology, Korea

ABSTRACT: Understanding behavior of soil may contribute to design retaining walls safely and efficiently. Therefore, in this study, behavior of ground by active and passive retaining walls was compared through finite-element analysis and laboratory model test using close range photogrammetric method. From the close range photogrammetry, deformation of sandy ground according to roughness and horizontal displacements of the model retaining wall was recorded and analyzed. The roughness was compared to interface factor. Also, vertical horizontal displacement and shear strain of the sandy ground were analyzed by PLAXIS 2D. The result of comparison between the numerical analysis and the laboratory model test shows good agreement. Consequently, the close range photogrammetry with image processing can be used to measure the ground deformation accurately. The relationship between the roughness of the wall and the interface factors can be used to design safely and efficiently.

1 INTRODUCTION

In this study, behavior of ground by the active and passive retaining wall models was predicted through the finite-element analysis and was investigated by the laboratory model test using close range photogrammetry. In the laboratory model test, roughness of the wall was set to two conditions: rough and smooth. Those were simulated by interface of numerical analysis. And, inverse analysis through the relationship between the interface element (virtual thickness factor, R_{inter}) and roughness of the wall was carried out. The interface was a key role in the simulation of ground and should be considered to design ground structures.

2 MODEL TEST AND MEASUREMENT

2.1 *Model tests*

For understanding ground behavior associated with horizontal displacement of the wall and its roughness laboratory model tests were carried out. The retaining wall model container was set to 1000 mm × 1000 mm size (Fig. 1). First the passive retaining wall model was prepared. Initial condition of the wall was set as shown in Fig. 2. In contrast, the active retaining wall was set (Fig. 3). Roughness of the wall was made by sandpaper. The sandpaper was attached in front of the wall for simulation of rough condition and the smooth condition didn't attached. Next, the ground was set. For measuring ground deformation aluminum rods (Fig. 4) were put into the sandy soil. The sand was piled up into 100 mm in height. In the sand, aluminum

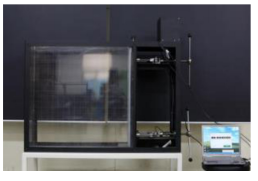

Figure 1. Retaining wall container.

Figure 2. Passive wall model.

rods were laid to spacing 100 mm. Observation of the passive retaining wall model test was required for 33 target points and 16 control points. And the active retaining model wall is required for 49 target points and same control point as the passive retaining model wall. The 16 control points regarding as reference points are attached on the surface of steel frame.

2.2 *Measurement*

For measurement of the active retaining wall, the wall was set to its original position and named Epoch_0 (initial stage) Next the wall moved with displacement from 1 mm to 2 mm. Each displacement condition was named from Epoch_1 to Epoch_5. Those

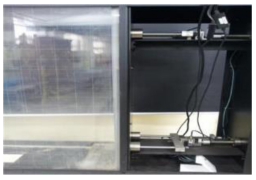

Figure 3. Active wall model.

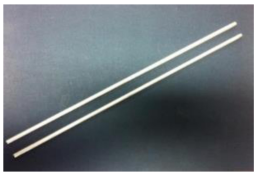

Figure 4. Aluminum rods.

(a) Camera

(b) Lens

(c) Flashlight

(d) Tripod

Figure 5. DSLR camera.

Table 1. Specification of Canon EOS 5D Mark II.

Model	Canon EOS 5D Mark II
Form	DSLR (Digital Single Lens Reflex)
Image sensor	36 × 24 mm
Pixel size	6.4 micron
Picture size	5616 × 3744 pixel
Lens	F = 50 mm, F = 1.4

were observed by DSLR (Digital Single Lens Reflex) camera (Fig. 5). Specification of DSLR camera is summarized in Table 1. Measurement of the passive retaining wall was set to opposite direction of the active retaining wall.

Images were obtained by the image processing. Locations of target points are different for each Epoch. But, those can be designated as the same number of points. These target points are measured by the fixed 16 control points. The target points represent for soil

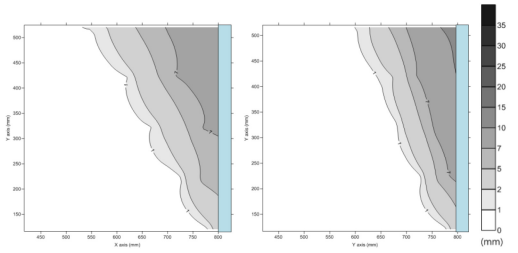

(a) Rough/5mm displacement (b) Smooth/5mm displacement

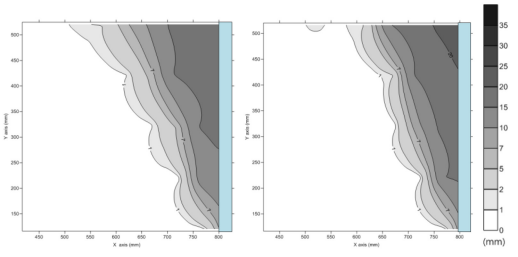

(c) Rough/10mm displacement (d) Smooth/10mm displacement

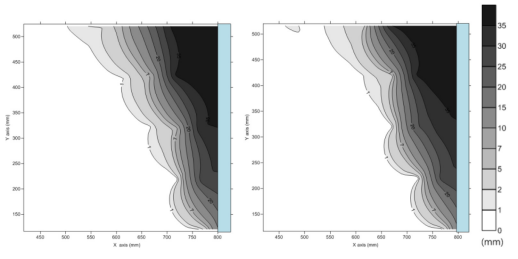

(e) Rough/20mm displacement (f) Smooth/20mm displacement

Figure 6. Vertical displacement contours of active retaining wall.

identified by image processing. Detailed explanation of close range photogrammetry method and image processing were introduced by Lee (2006), Lee et al. (2012) and Lee et al. (2013).

3 RESULTS FROM IMAGE PROCESSING

3.1 *Result of the active retaining wall model*

Image processing results of the active retaining wall are as in the following: vertical and horizontal displacements are generated. Figs. 6 and 7 show the vertical and horizontal displacement contours according to wall roughness and horizontal displacements. Each pictures show large displacement in front of the retaining wall when wall is smooth condition.

3.2 *Result of the passive retaining wall model*

Figs. 8 and 9 show the vertical and horizontal displacement contours for the passive retaining wall. Displacement concentrations at the near wall face are similar to the active retaining wall.

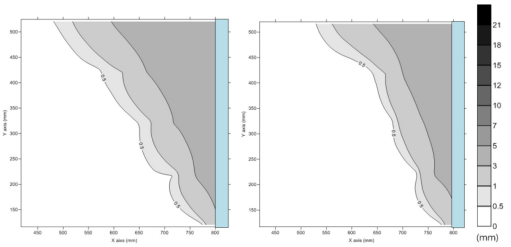

(a) Rough/5mm displacement (b) Smooth/5mm displacement

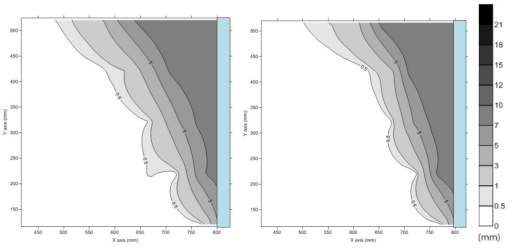

(c) Rough/10mm displacement (d) Smooth/10mm displacement

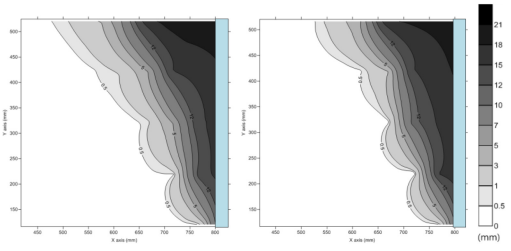

(e) Rough/20mm displacement (f) Smooth/20mm displacement

Figure 7. Horizontal displacement contours of active retaining wall.

4 NUMERICAL ANALYSIS

4.1 *Modeling and material conditions*

The numerical analysis program PLAXIS 2D was used. Boundary condition size is 1000 mm × 1000 mm Material conditions of sand and steel plate are given in Table 2. Displacements of wall are applied to step by step: 1 mm, 3 mm, 5 mm, 10 mm, 20 mm. Fig. 10 shows displacement control of the retaining wall and boundary conditions. Fig. 11 shows FE mesh. Also, two interface factors are considered. First, virtual thickness factor is used for interface factor between the ground and the wall. Second, Rinter (strength reduction factor) is used as before. These interface factors was compared to roughness of the wall. Detailed research of the interface explained by Goodman et al. (1968), Ghaboussi et al. (1973), Carol and Alonso (1983), Wilson (1977), Desai et al. (1984), Beer (1985). Francavailla and Zienkiewicz (1975), Sachdeva and Ramakrishnan (1981), Katona (1983) and Lai and Booker (1989).

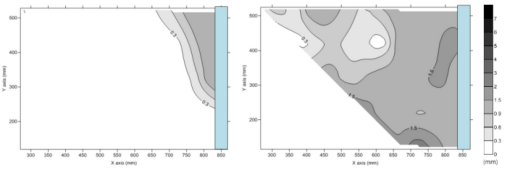

(a) Rough/5mm displacement (b) Smooth/5mm displacement

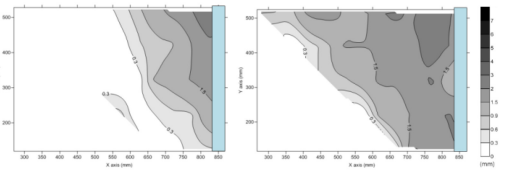

(c) Rough/10mm displacement (d) Smooth/10mm displacement

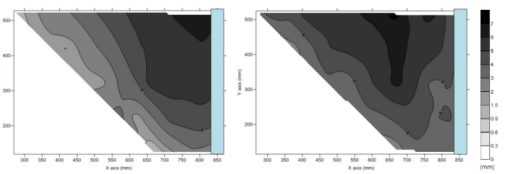

(e) Rough/20mm displacement (f) Smooth/20mm displacement

Figure 8. Vertical displacement contours of passive retaining wall.

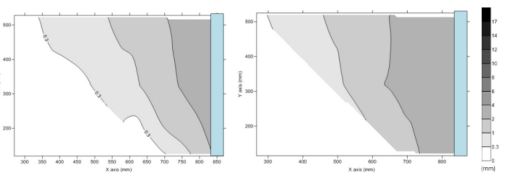

(a) Rough/5mm displacement (b) Smooth/5mm displacement

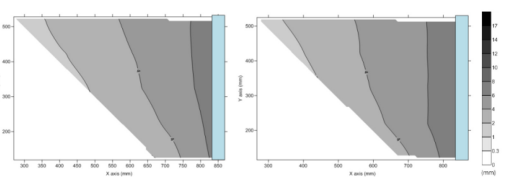

(c) Rough/10mm displacement (d) Smooth/10mm displacement

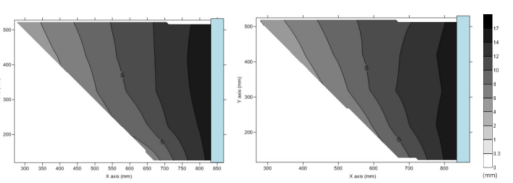

(e) Rough/20mm displacement (f) Smooth/20mm displacement

Figure 9. Horizontal displacement contours of passive retaining wall.

4.2 *Result of numerical analysis: the active condition*

Figs. 12 and 13 show the vertical and horizontal displacement contours according to interface conditions

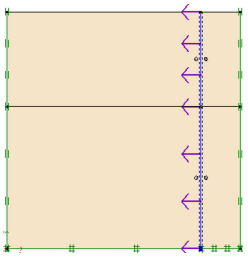

Figure 10. Boundary condition.

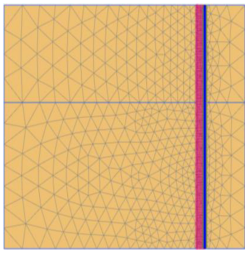

Figure 11. FE mesh.

Table 2. Input parameters in FE analysis.

Soil		Wall	
E (kN/cm^2)	4.0	EA (kN/cm)	5400
C (kN/cm^2)	0.1	EI (kN/cm^2/cm)	364.5
ν	0.35	ν	0.35
Φ (°)	32.0	w (kN/cm/cm)	0.0212
Ψ (°)	0.0		
γ (kN/cm^3)	0.000017		

E: Young's modulus, c: Cohesion, ν: Poisson's ratio, Φ': Angle of shearing resistance, Ψ: Dilation angle, γ: Unit weight of soil.

of the active retaining wall. The interface conditions deduced similar results from the image processing. Virtual thickness factor and Rinter are applied from 0.1 to 1.0 respectively. As a result, when the virtual thickness factor 0.1 a similar displacement distribution was appeared. In contrast R_{inter} shows same result in each condition. So, R_{inter} was applied as a basic value 0.1 in PAXIS 2D program. Figs. 12 and 13 show similar result from the image processing. But, the large displacement is generated when the interface isn't considered.

4.3 *Result of numerical analysis: passive condition*

Figs. 14 and 15 show the vertical and horizontal displacement contours according to interface conditions of the passive retaining wall. The interface conditions of the active retaining wall are equally applied to the passive retaining wall. Figs. 15 and 16 show the similar pattern from the image processing. When the interface factors are not considered, the greater vertical and horizontal displacements are generated.

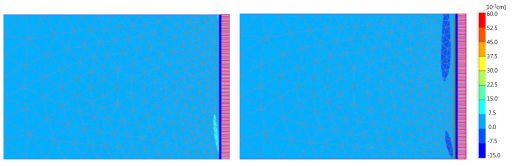

(a) Without interface/5mm displacement (b) With interface/5mm displacement

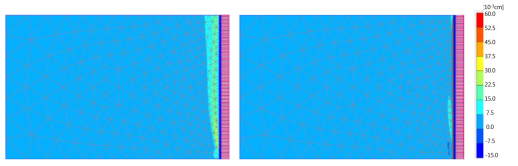

(c) Without interface/10mm displacement (d) With interface/10mm displacement

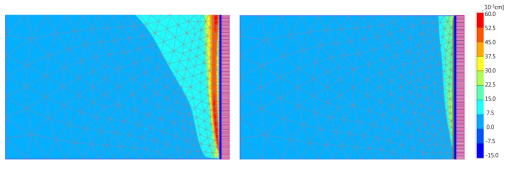

Figure 12. Vertical displacement of active retaining wall contours.

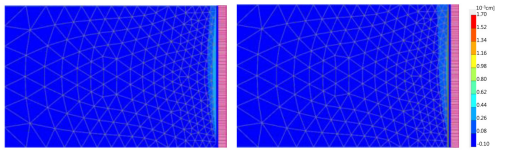

(a) Without interface/5mm displacement (b) With interface/5mm displacement

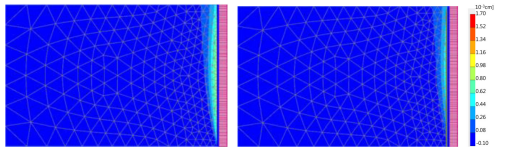

(c) Without interface/10mm displacement (d) With interface/10mm displacement

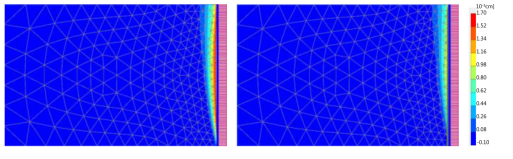

(e) Without interface/20mm displacement (f) With interface/20mm displacement

Figure 13. Horizontal displacement of active retaining wall contours.

4.4 *Shear strain and failure envelope*

In this study, shear strain and failure envelope are compared to Rankine's theory (1857). Similarly, in the model test, failure envelope was observed by black sand that is set between sand. Fig. 16 shows failure envelope of active and passive retaining walls. Also, shear strain was generated by numerical analysis (Fig. 17). This study shows a similar failure envelope compared to Rankine's theory (1857) from both the model test and numerical analysis.

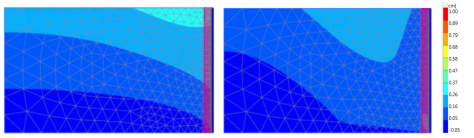

(a) Without interface/5mm displacement (b) With interface/5mm displacement

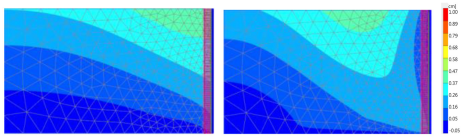

(c) Without interface/10mm displacement (d) With interface/10mm displacement

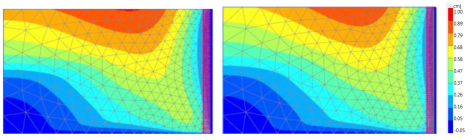

(e) Without interface/20mm displacement (f) With interface/20mm displacement

Figure 14. Vertical displacement of passive retaining wall contours.

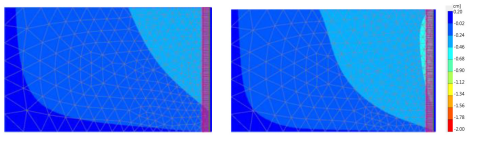

(a) Without interface/5mm displacement (b) With interface/5mm displacement

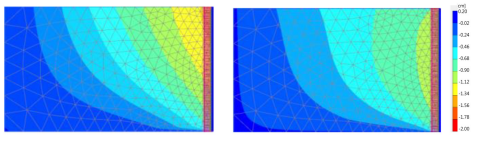

(c) Without interface/10mm displacement (d) With interface/10mm displacement

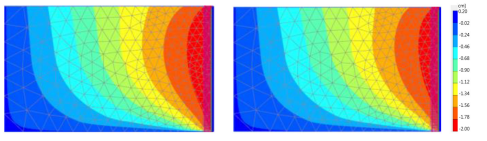

(e) Without interface/20mm displacement (f) With interface/20mm displacement

Figure 15. Horizontal displacement of passive retaining wall contours.

5 CONCLUSIONS

The authors have investigated behavior of ground by the passive and active retaining wall models using close range photogrammetry and image processing. And, numerical analysis predicts appropriate the interface factors with the inverse method. Also, laboratory model test shows the failure envelopes that are similar to Rankine's theory (1857). Those are also observed by numerical analysis. These findings are summarized as follows:

(1) The laboratory model test simulates behavior of ground by active and passive retaining walls. The roughness of the wall is two types: rough and smooth. Accordingly, results from image processing show that the smooth condition generates greater displacement than rough condition.

(2) Results from numerical analysis show that without interface condition is greater displacement than with interface. When the virtual thickness factor is 0.1, the displacement pattern is similar to the model test But, R_{inter} does not affect to the displacement contribution

(3) The relationship between the roughness of the wall and the interface factors can be used to design safely and efficiently. Also, close range photogrammetry is useful in investigation of ground.

(4) Failure envelopes are observed in the laboratory model tests. These failure envelopes are similar to both Rankine's theory (1857) and the numerical analysis.

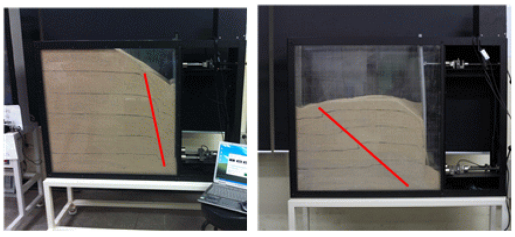

(a) Active retaining wall (b) Passive retaining wall

Figure 16. Failure envelopes from model test.

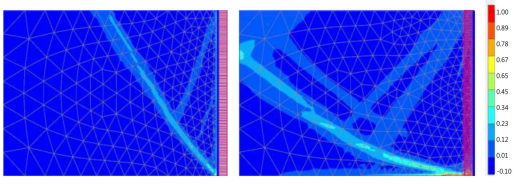

(a) Active retaining wall (b) Passive retaining wall

Figure 17. Shear strains from numerical analysis.

ACKNOWLEDGEMENT

This study was supported by Basic Science Research Program through the National Research Foundation of Korea (NRF-2013R1A1A2005101).

REFERENCES

Beer, G. (1985). "An isoparametric joint/interface element for finite element analysis", Int. Jnl. 5th Int. Num. Meth. Eng., Vol. 21, pp. 585–600.

Carol, I. and Alonso, E. E. (1983). "A new joint element for the analysis of fractured rock", 5th Int. Congr. Rock Mech., Melbourne, Vol. F, pp. 37–42.

Desia, C. S., Zaman, M. M., Lightner, J. G. and Siriwardane, H. J. (1984). "Thin-layer element for interfaces and

joints", Int. Jnl. Num. Anal. Meth. Gemech., Wol. 8, pp. 935–950.
Francavila, A. and Zienkieviczs, O. C. (1975). "A note on numerical computation of elastic contact problems", Int. Jnl. Num. Meth. Eng., Vol. 9, pp. 913–924.
Ghaboussi, J., Wilson, E. L. and Isenberg, J. (1973). "Finite element for rock joint interfaces", ASCE, SM10, Vol. 99, pp. 833–848.
Goodman, R. E., Taylor, R. L. and Brekke, T. L. (1968). "A model for the mechanics of jointed rock", ASCE, SM3, Vol. 94, pp. 637–659.
Katona, M. G. (1983). "A simple contact-friction interface element with application to buried cuverts", Int. Jnl. Num. Anal. Meth. Gemech., Vol. 7, pp. 371–384.
Lai, J. Y. and Booker, J. R. (1989). "Application of discrete Fourier series to the finite element stress analysis of axi-symmetric solids", Int. Jnl. Num. Meth. Eng., Vol. 31, pp. 619–647.
Lee, Y. J., Bassett, R. H. (2006). "Application of a photogrammetric technique to a model tunnel", Tunnelling and Underground Space Technology 21 (3–4), 370.
Lee, C. N., Oh, J. H. (2012). "A Study on Efficient Self-Calibration of a Non-Metric Camera for Close-range Photogrammetry" Journal of Korean Society of Surveying, Geodesy, Photogrammetry and Cartography, 30, Vol. 6–1, pp. 511–518.
Lee, C. N., Oh, J. H. (2013). "Measurement of Soil Deformation around the Tip of Model Pile by Close-Range Photogrammetry", Journal of Korean Society of Surveying, Geodesy, Photogrammetry and Cartography, 31, Vol. 2, pp. 173–180.
PLAXIS V8 (2006). Reference manual.
Rankine, W. M. J. (1857). "On Stability on Looose Earth," philosophic Transactions of Royal Society, Lundon, Part I, 9–27.
Sachdeva, T. D. and Ramakrishnan, C. V. (1981). "A finite element solution for the two dimensional elastic contact problem", Int. Jnl. Num. Meth. Eng., Vol. 17, pp. 1257–1271.
Wilson, E. L. (1977). "Finite elements for foundatios, joints and fluids", Chapter 10 in Finite elements in Geomechanics, Edt. Gudehus, John Wiley & Sons.